Early-warning signals of critical transition: Effect of extrinsic noise

Shanshan Qin[1] and Chao Tang[1,2,*]

[1]*Center for Quantitative Biology, Peking University, Beijing 100871, China*

[2]*School of Physics and Peking-Tsinghua Center for Life Sciences, Peking University, Beijing, 10087, China*

(Received 8 January 2018; published 13 March 2018)

Complex dynamical systems often have tipping points and exhibit catastrophic regime shift. Despite the notorious difficulty of predicting such transitions, accumulating studies have suggested the existence of generic early-warning signals (EWSs) preceding upcoming transitions. However, previous theories and models were based on the effect of the intrinsic noise (IN) when a system is approaching a critical point, and did not consider the pervasive environmental fluctuations or the extrinsic noise (EN). Here, we extend previous theory to investigate how the interplay of EN and IN affects EWSs. Stochastic simulations of model systems subject to both IN and EN have verified our theory and demonstrated that EN can dramatically alter and diminish the EWS. This effect is stronger with increasing amplitude and correlation time scale of the EN. In the presence of EN, the EWS can fail to predict or even give a false alarm of critical transitions.

DOI: 10.1103/PhysRevE.97.032406

I. INTRODUCTION

Complex dynamical systems exhibit critical transitions when external and/or internal conditions drive the system to pass a critical point. Such transitions are often catastrophic and irreversible. Examples include collapse of ecosystems [1–3], rapid climate change [4–6], crash of financial markets [7], and deterioration of medical conditions [8–10]. Anticipating and averting such events is highly desirable due to their obvious importance. Recently, many studies have proposed that certain impending critical transitions can in principle be identified through generic signs called the early-warning signals (EWSs) regardless of their underlying details [11–13]. Most of the proposed EWSs are based on the increasing trend of some summary statistics, such as the rising of variance [14–16], autocorrelation coefficient at lag-one [$R(1)$] [17,18], skewness [14,19], and the Pearson correlation coefficient (ρ) [20,21]. The idea behind previous theory is that critical transitions correspond to dynamical bifurcations, especially the fold bifurcation (or saddle-node bifurcation). Systems that are near critical points recover back to their equilibrium much slower after perturbation, known as critical slowing down (CSD) [22–24]. In the presence of small noise, the EWS is a direct consequence of CSD [12].

Despite their strong theoretical underpinning, these EWSs have only been tested in a few controlled experiments [14,25–27], and failed when applied to field data [28–30], raising debates of their generality and robustness [31]. Understanding the failure and evaluating the performance of EWSs are essential for its practical applications. Most of the previous studies only considered the intrinsic noise (IN), which arises from, e.g., the stochastic birth and death of species of low numbers in cells or ecosystems. The effect of the pervasive environmental fluctuations, or the extrinsic noise (EN), has been largely ignored. EN has been demonstrated to have a drastic effect on dynamical systems [32,33]. For example, EN can enhance regular behavior [34], such as noise-induced transitions [35–37], stochastic resonance [38], and pattern formations [34].

The validation of previous EWS theory relies on the small IN assumption, which is true for large enough systems since IN scales inversely with the system size. However, EN does not have such property and cannot be neglected even in the thermodynamic limit. Generally speaking, EN is shared by all components in a system, introducing inherent correlations among them. How EN interacts with IN to alter the stochastic dynamics and influences the performance of EWS remains largely unknown.

In this paper, we incorporate EN in dynamical systems that exhibit critical transitions and systematically examine its impact on EWSs. We first formulate an equation that quantitatively describes the effect of EN on EWS by extending previous theory. We then applied our theory to analyze the impact of EN on several simple models subject to various types of EN. The analytical results were tested and compared with numerical simulations (Appendixes B and C). Our results suggest that EN can dramatically diminish EWSs, and this effect increases with the magnitude and correlation time scale of the EN, as well as the system size. We also find that for certain systems, an EWS can give false alarm of critical transitions as a result of EN. For time sequence data, we find that even under the minor strength of EN, the EWS fails to identify the critical transition. Our results demonstrate the complex effect of EN on EWSs.

II. THEORY

Consider a general dynamical system of N variables $\mathbf{x} = (x_1, x_2, \ldots, x_N)$ whose deterministic behavior is described by $\dot{\mathbf{x}} = f(\mathbf{x}, \theta)$, where θ represents the set of parameters. When noise is relatively small, its stochastic behavior at steady state

*tangc@pku.edu.cn

can be generally studied using the linear noise approximation (LNA) method [39–42], described by the following stochastic differential equation (SDE),

$$d\mathbf{x}(t) = A\mathbf{x}(t)dt + Bd\mathbf{w}(t), \tag{1}$$

where the deviation from the steady state $\delta\mathbf{x} \equiv \mathbf{x}(t) - \mathbf{x}^*$ has been rewritten as $\mathbf{x}(t)$ for simplicity. A is the Jacobian matrix of the corresponding deterministic dynamics at the steady state, $\mathbf{w}(t)$ is an M-dimensional Wiener process, and B is an $N \times M$ matrix which determines the amplitude of the noise. At the steady state, the covariance matrix of variable fluctuations C, Jacobian matrix A, and the diffusion matrix $D \equiv BB^T$ follows [41]

$$AC + CA^T + D = 0, \tag{2}$$

and the correlation function $G(\tau) \equiv \langle \mathbf{x}(t)\mathbf{x}^T(t+\tau)\rangle$ is

$$G(\tau) = Ce^{A^T\tau}. \tag{3}$$

Equations (2) and (3) are the foundation of the previous EWS theory, which lead to several widely used EWSs, including divergence of variance, enhancement of ρ (to 1 or -1) and enhancement of $R(1)$ (to 1). To see this explicitly, consider the zero-eigenvalue bifurcation ($\lambda \to 0$) of a single-variable system with small noise: We have $\lambda C + C\lambda = D$; hence the variance of the variable fluctuation $D/|2\lambda|$ diverges and $R(1) \to 1$. For multivariable systems, variables that constitute the zero-eigenvector exhibit divergence of variance and increase of $R(1)$, and fluctuations of these variables get strongly correlated or anticorrelated [21].

We now extend the above theory to more general situations with both IN and EN. A conventional way to incorporate EN is through fluctuating parameters [43,44], usually modeled as an Ornstein-Uhlenbeck process [32,45–47],

$$\dot{\theta}_t = (\theta_0 - \theta_t)/\tau_c + \sqrt{2\sigma_e^2/\tau_c}\xi(t), \tag{4}$$

where τ_c is the correlation time scale, σ_e^2 is the variance of EN, and $\xi(t)$ is a unit Gaussian white noise with $\langle \xi(t)\xi(t')\rangle = \delta(t-t')$. Notice that an N-variable system subject to n-variate EN is equivalent to an $N+n$ variable system with only IN. Denoting its Jacobian matrix, covariance matrix, and diffusion coefficient matrix as $\tilde{A}, \tilde{C}, \tilde{D}$, and applying the LNA method [39–42], we have

$$\tilde{A}\tilde{C} + \tilde{C}\tilde{A}^T + \tilde{D} = 0, \tag{5}$$

where

$$\tilde{A} = \begin{bmatrix} A & \alpha^T \\ 0 & \beta \end{bmatrix}, \quad \tilde{C} = \begin{bmatrix} C' & C_2 \\ C_2^T & C_3 \end{bmatrix}, \quad \tilde{D} = \begin{bmatrix} D & 0 \\ 0 & D_E \end{bmatrix}.$$

$\alpha = \partial f(x,\theta_t)/\partial\theta_t$ at $(\mathbf{x}^*,\theta_0)$, which is an $N \times n$ matrix, represents the coupling of EN to the internal system. β is a diagonal matrix with diagonal elements $[-1/\tau_c^{(1)}, \ldots, -1/\tau_c^{(n)}]$, where $\tau_c^{(i)}$ is the correlation time scale of the ith EN. C_2 represents the covariance between internal dynamical variables and EN variables, C_3 is the covariance of EN, D_E is the diffusion matrix associated with Eq. (4). Our goal is to obtain C', the covariance matrix of the internal dynamical variables after introducing EN. Generally, it is difficult to solve for C' explicitly from Eq. (5). A conventional approach is to use the matrix vectorization and Kronecker product method [48]. The vectorized form of $\tilde{C}$, defined as the stacking of its columns, can be solved as

$$V_{\mathrm{vec}}(\tilde{C}) = -(\mathbb{I}_n \otimes \tilde{A} + \tilde{A} \otimes \mathbb{I}_n)^{-1} V_{\mathrm{vec}}(\tilde{D}), \tag{6}$$

where $\mathbb{I}_n$ is the unit matrix and $\otimes$ is the Kronecker product of the matrix. The impact of EN on EWSs is obtained by comparing $\tilde{C}$ and C. For one-variable or two-variable systems, it has a more concise form and the explicit difference between $\tilde{C}$ and C can be obtained (see Appendix A).

III. RESULTS

A. EWSs in the presence of EN for single-variable system

We begin with a comprehensive analysis of the impact of EN on EWSs for a well-studied single-variable dynamical system, the insect outbreak model [49]. The evolution of the population of budworm in a forest is described by $\dot{x} = x - ax^2 - bx^2/(1+x^2)$. The first two terms represent logistic growth of the population, and the third term is due to predation by birds. This system can be either monostable or bistable depending on the values of a and b. In the monostable regime with high population density ($a = 0.05$, $b = 1.5$), we add EN to the growth rate (the coefficient of the first term). The steady state variance C′ with EN added is

$$C' = D/|2\lambda| + \sigma_e^2\alpha^2/|\lambda(\lambda+\beta)|, \tag{7}$$

where λ is the eigenvalue of the linearized system at steady state x^* (see Appendix A). The autocorrelation coefficient is

$$R(1) = e^{\lambda} + \frac{2\alpha^2\lambda\sigma_e^2(e^{\beta} - e^{\lambda})}{[D(\beta+\lambda) - 2\alpha^2\sigma_e^2](\beta-\lambda)}. \tag{8}$$

Equations (7) and (8) can be further simplified in two important limits: white EN and adiabatic EN.

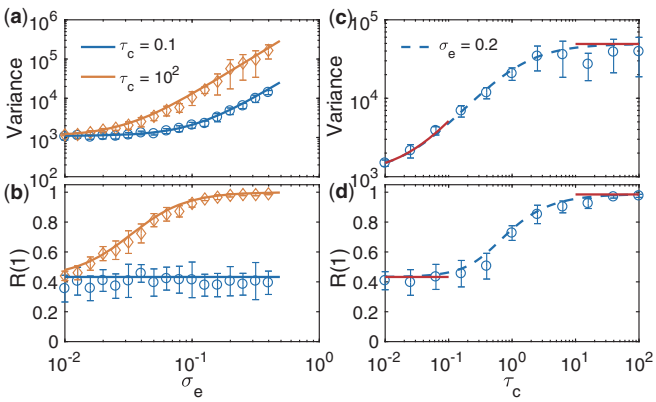

FIG. 1. Comparison of theory (lines) and simulation (symbols) for the insect outbreak model with $\Omega = 50$, $a = 1/20$, $b = 1.5$. (a,b) Total variance and $R(1)$ vs EN amplitude for white EN (blue) and adiabatic EN (orange). (c,d) Total variance and $R(1)$ vs EN correlation time scale with $\sigma_e = 0.2$, $\tau_c = 10$. The red solid lines show the theoretical results for white and adiabatic EN. Error bars are standard deviation of 50 simulations.

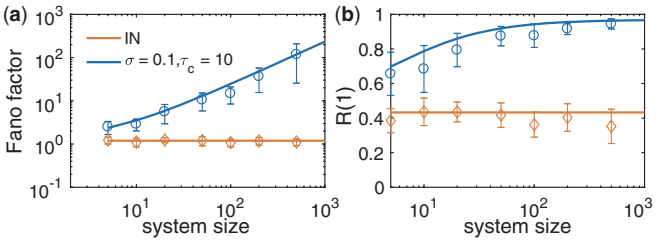

FIG. 2. Comparison of theory (lines) and simulation (symbols) for system-size-dependent effect. Total variance (a) and $R(1)$ (b) vs system size for IN-only (blue) and with-EN (orange) cases in the insect outbreak model (with $a = 1/20$, $b = 1.5$). Error bars are standard deviations of 50 simulations.

In the white noise limit, we have $\tau_c = -1/\beta \ll 1$, then $C' \approx C(1 + 2\alpha^2\sigma_e^2\tau_c/D)$. Thus the variance increases by a factor that scales with σ_e^2, α^2, and τ_c. The second term in Eq. (8) vanishes, so $R(1) = e^{\lambda}$. Hence, white EN does not change the autocorrelation function [see Figs. 1(a)–1(b)].

In the adiabatic limit, we have $\tau_c = -1/\beta \gg 1$, then $C' \approx C(1 + 2\alpha^2\sigma_e^2/D|\lambda|)$, and $\mathrm{R}(1) = e^{\lambda} + (1 - e^{\lambda})/(1 + \epsilon)$ with $\epsilon \equiv |D\lambda|/2\alpha^2\sigma_e^2$. The fold change of variance and $R(1)$ is determined mainly by ϵ; when $\epsilon \ll 1$, C' diverges, and $R(1) = 1$ [see Figs. 1(c)–1(d)].

Generally, the relative amplitude of IN scales with $1/\sqrt{\Omega}$, where Ω is the "system size." In contrast, EN does not have this property. In the above model, $\alpha \propto \Omega$, indicating that EN scales with Ω^2. Hence, EN is dominant for large systems and $R(1)$ approaches 1 (see Fig. 2). Taken together, the steady state value of variance and $R(1)$ strongly depend on EN, and can be very large even if the system is far away from the critical point.

B. Toggle switch motif subjects to IN and EN

We now apply our theoretical framework to a well-studied two-variable system, the toggle switch model: two transcription factors A and B suppress the expression of each other by binding to the corresponding promoter regions. Denoting the concentration of proteins as x and y, the coarse-grained dimensionless deterministic equations describing this system are [50] $\dot{x} = a_1[a_0 + (1 - a_0)/(1 + y^{n_1})] - x$ and $\dot{y} = a_2[a_0 + (1 - a_0)/(1 + x^{n_2})] - y$. The first term on the right-hand side (RHS) of each equation represents protein synthesis, consisting of a basal rate a_0 and a Hill-function form regulated rate. a_1 and a_2 represent the maximum expression rates; n_1 and n_2 are Hill coefficients. The second terms on the RHS represent the degradation of proteins. The qualitative dynamic properties of this system have been well studied. In some parameter regions, it exhibits bistability, where the expression level of A (or B) can be either high or low depending on the initial state of the system.

We simultaneously incorporated EN into the degradation rates of proteins A and B according to Eq. (4). We compared the aforementioned three EWSs: variance (in terms of the Fano factor), ρ, and $R(1)$, when this system is driven toward a transition point. For each control parameter a_1, EWSs are estimated from 50 long stationary trajectories. Consistent with previous theory (Fig. 3, black lines), with very small EN, both our simulation (Fig. 3, blue triangles) and the theory

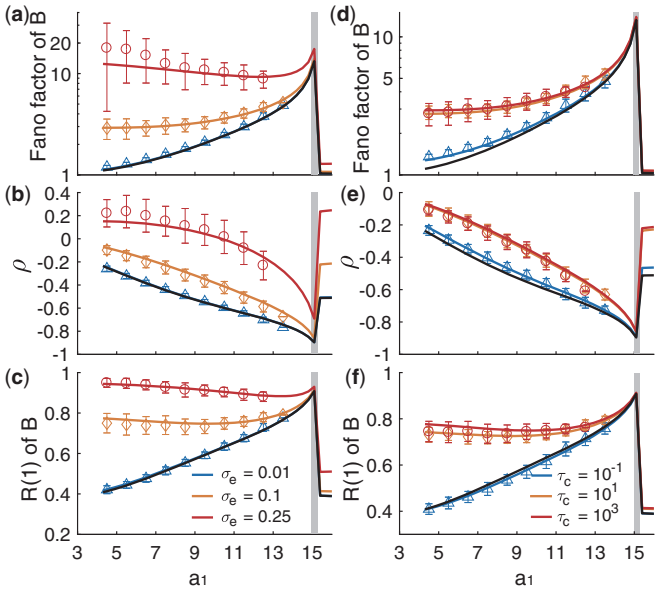

FIG. 3. EWSs in a toggle switch model subject to various ENs: theoretical (solid lines) and simulation (symbols) results. Shown are the Fano factor of gene B, the Pearson correlation coefficient between A and B, and $R(1)$ of B, subject to different amplitudes of EN (a–c) and different correlation time scales of EN (d–f). At each a_1, numeric results are estimated from stationary long-time trajectories. Shadowed areas indicate the critical point. Parameters values are $n_1 = n_2 = 2$, $a_2 = 10$, $a_0 = 0.05$, $\Omega = 20$. In (a–c), $\tau_c = 100$, in (d–f), $\sigma_e = 0.1$. Error bars are standard deviations of 50 simulations.

(Fig. 3, blue line) show that EWSs dramatically increase prior to the upcoming critical transition. However, the rise of the Fano factor with respect to a_1 becomes feeble as the amplitude of EN increases (denoted by different colors). With stronger EN, its trend even becomes nonmonotonic, decreasing first and only increasing at the very vicinity of the critical point [Fig. 3(a)]. ρ and $R(1)$ exhibit similar behavior; both are dramatically diminished with increasing amplitude of EN [Figs. 3(b) and 3(c)]. These can be interpreted as a complex interaction between the internal time scale and the time scale of EN. When the system is far away from the critical point, EN is dominant due to its slow time scale ($\tau_c = 100$), while at the very vicinity of the critical point, the internal time scale surpasses that of EN and IN becomes dominant.

We also studied the effect of correlation time scale of EN on EWSs. With increasing correlation time scale, the increase of EWSs with respect to the control parameter (as it approaches the critical point) decreases [Figs. 3(d)–3(f)].

C. False alarm of critical transition

Next, we study how EN may give a false alarm in systems with no critical transition. Our model is the common two-gene negative feedback loop: transcription factor A promotes the expression of B, while B inhibits the expression of A. The deterministic equations are $\dot{x} = a_0 + (1 - a_0)k_1^n/(k_1^n + y^n) - x$, $\dot{y} = a_0 + (1 - a_0)x^n/(k_2^n + x^n) - y$. Expression level of gene B at steady state increases continuously with the control parameter k_1 [Fig. 4(a)]. Without EN, the Fano factor of B

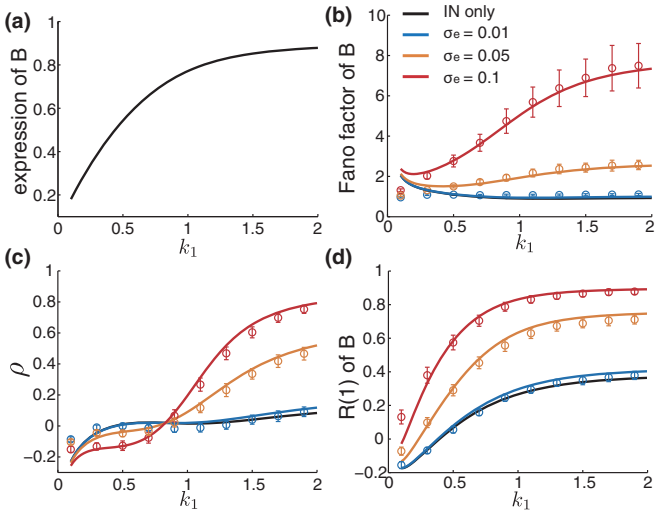

FIG. 4. EWSs can give a false alarm in a simple negative feedback loop model with no critical transition. (a) Steady state expression level of gene B as a function of parameter k_1. (b–d) When subjected to EN, EWSs rise rapidly with the increase of control parameter k_1. The solid lines are theoretical results based on Eq. (6) and symbols with error bars are the mean of 50 stochastic simulations. Parameter values are $a_0 = 0.05$, $k_2 = 0.5$, $n = 3$, $\Omega = 500$.

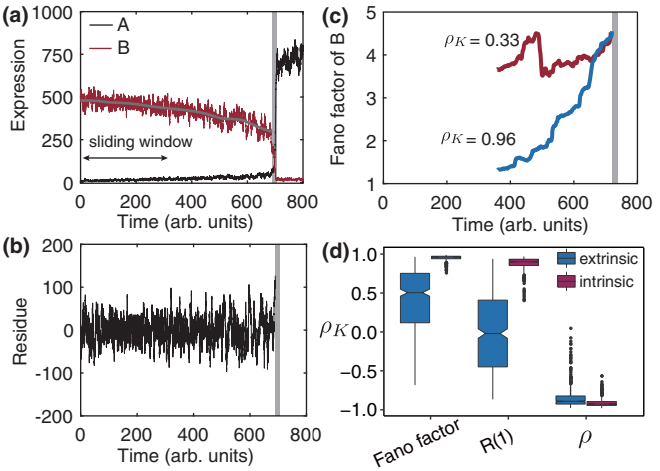

FIG. 5. Comparison of EWSs derived from time series of the toggle switch model with and without EN. (a) Control parameter a_1 increases linearly with time from 2 to 18 in a time window of 1000. Trajectories of expression level of A and B with only IN are shown. Gray band marks the transition events. The smooth solid gray line through the time series is a Gaussian kernel smoothing function used to filter out longer-term trends. The arrow marks the width of the sliding window used to calculate EWSs. (b) Residue after subtracting the average of the Gaussian kernel. (c) Example of estimated Fano factor from (b) prior to the critical transition. Purple line: IN only. Blue line: with EN ($\sigma_e = 0.1$, $\tau_c = 10$). (d) Including EN dramatically diminishes two EWSs, but the Pearson correlation coefficient is relatively robust. Box plot of Kendall's rank correlation coefficient (ρ_K) of 500 trials.

does not increase much with k_1, and the Pearson correlation coefficient between A and B, and $R(1)$ of B remain close to 0 as k_1 increases. However, all of the three EWSs rise dramatically with the increase of k_1 when EN is imposed, especially when EN is large [Figs. 4(b)–4(d), solid lines]. This simple example demonstrates that when a system is subject to EN, conventional EWSs may give a false alarm of critical transition.

D. Early-warning signals based on time series data

Most natural systems can only afford a small number of samples and/or limited times of observation, such as a single trajectory of system state driven by a slowly changing control parameter. Previous studies have suggested EWSs can precede critical transition even using a single time series, provided that the control parameter changes relatively slowly and IN is small [12,17].

We next examined the effect of EN on EWS estimated from single trajectories in the toggle switch model. When control parameter a_1 changes gradually and drives the system past the critical point, the system jumps to the alternative state [shadow area in Fig. 5(a)]. To calculate time-dependent EWS, we used a conventional sliding window method [16]. First, we subtract a Gaussian kernel smoothing function (thick gray solid lines) from the trajectory to filter out trends on a large time scale and the residues were used for further analysis [Fig. 5(b)]. Then, a sliding window was used for the residues up to the transition point to estimate EWS.

Consistent with previous studies, all the three EWSs show a strong increase prior to the critical transition when there is no EN. The trend is quantified by the Kendall's rank correlation coefficient ρ_K a larger value of ρ_K indicates a stronger trend. However, imposing medium strength of EN dramatically impairs the trend of the Fano factor and $R(1)$. The trend of ρ is relatively robust but its absolute value is smaller compared with the IN-only situation [Fig. 5(d)]. Since the exact time when the system jumps to the alternative state differs from trial to trial, we simulated 500 such trajectories with and without EN. The trends of EWSs prior to the transition are summarized in Fig. 5(d). The values of ρ_K are all centered around 1 or -1 when only IN is present, indicating a very strong trend of increase. With EN included, the distribution of ρ_K is much broader and has a small average value, indicating that EWSs do not have a defined increasing trend before the transition. This result demonstrated that for time series data, even minor EN can drastically diminish EWSs.

IV. CONCLUSIONS

We have extended the previous linear noise approximation theory to dynamical systems subject to both IN and EN, allowing us to explore the influence of EN on the EWS under rather general conditions. Our theory has been tested on simple models subject to various forms of EN. Our results suggest that EN could largely diminish an EWS when a dynamical system is approaching a critical point. This effect becomes stronger with the increase of magnitude and correlation time scale of EN, as well as the increase of system size. The drastic effect of EN on EWS is attributed to its nonlinear coupling to the internal dynamics and its relatively slow time scale. They interact synergistically to produce nontrivial fluctuations of the system. We caution that EN could be an important source to cause false alarms and false negative results when using EWSs

to identify or predict critical transitions in natural systems. Our work also contributes toward a more general framework to study IN and EN in dynamical systems.

Note that not all regime shifts belong to critical transitions [51] and different types of regime shifts can be classified according to several time scales [52]. The realization that certain regime shifts or critical transitions in principle can be predicted represents a substantial step forward. Nevertheless, extracting reliable EWSs from real data can be challenging. Previous works seldom characterized the robustness and sensitivity of EWSs [28]. In this study, we demonstrated that EN could be one of the important reasons that causes EWS theory to fail. As has already been suggested, model-based approaches, treating individual systems separately, could potentially alleviate such challenge [28,31].

In this study, as well as in most of the previous studies on EWSs, the systems considered are spatially homogeneous and well mixed. Many real systems have limited dispersion (diffusion) rate and are spatially inhomogeneous [53,54]. Noise in spatially extended systems is known to have profound effects [55], such as noise-induced transition [35], stochastic resonance [38], and pattern formation [34,56]. As has been well studied in both equilibrium and nonequilibrium systems, spatial heterogeneity generally changes abrupt transitions (first order) to continuous transitions [57–59]. Furthermore, spatial disorder can induce a broad region near the transition point called the "Griffith phase" where generic scale-free behavior can be observed [60,61]. It has been suggested that some emergent spatiotemporal patterns could be indicators of tipping points [62–66]. Future works that systematically explore the influence of spatial heterogeneity, internal noise, and environmental fluctuations on the behavior of dynamical systems will certainly deepen our understanding on catastrophic transitions.

Without knowing the dynamical rules and assessment of various factors that could affect the systems' behavior, such as the strength of EN, EWSs are not robust indicators of critical transitions. Due to the complex interplay of EN with internal nonlinear dynamics, EN and IN can be separated only in very special situations which usually do not hold [43,67,68]. Future studies in this area should also develop robust methods to assess the EN level in a dynamical system in order to have better quantifications of EWSs.

ACKNOWLEDGMENTS

We thank Xiaojing Yang, Xiaochan Xu, Chang Chang, Jingxiang Shen, Zongmao Gao, Qianyi Li, and Shaopeng Wang for helpful discussions and comments. The work was supported by the Chinese Ministry of Science and Technology (Grant No. 2015CB910300) and the National Natural Science Foundation of China (Grant No. 91430217).

APPENDIX A: LINEAR NOISE APPROXIMATION FOR SYSTEM WITH EXTRINSIC NOISE

Here we use the linear noise approximation method [39,41,69] to derive Eq. (6) in the main text. The techniques we used are matrix vectorization and the Kronecker product [48]. For a matrix $B \in R^{m\times n}$ with column $(b_1, b_2, \ldots, b_n)$, its vectorization is defined as the stacking of columns,

$$V_{\mathrm{vec}}(B) = \begin{pmatrix} b_1 \\ \vdots \\ b_n \end{pmatrix} \in R^{nm}. \tag{A1}$$

For matrix A, X, B with proper dimensions, we have the following identity,

$$V_{\mathrm{vec}}(AXB) = (B^T \otimes A)V_{\mathrm{vec}}(X), \tag{A2}$$

where $\otimes$ is the Kronecker product. Equation (5) in the main text is also called the Lyapunov matrix equation, which has a unique solution since all the eigenvalues of A are smaller than 0 [48]. Inserting the identity matrix on the left side of Eq. (5) and applying Eq. (A2) to it, we have

$$V_{\mathrm{vec}}(\tilde{A}\tilde{C} + \tilde{C}\tilde{A}^T) = -V_{\mathrm{vec}}(\tilde{D}), \tag{A3}$$

$$(I_n \otimes \tilde{A} + \tilde{A} \otimes I_n)V_{\mathrm{vec}}(\tilde{C}) = -V_{\mathrm{vec}}(\tilde{D}). \tag{A4}$$

We then get Eq. (6) in the main text.

$$V_{\mathrm{vec}}(\tilde{C}) = -(I_n \otimes \tilde{A} + \tilde{A} \otimes I_n)^{-1}V_{\mathrm{vec}}(\tilde{D}). \tag{A5}$$

While this form is easy to do numerical calculation, it does not explicitly show the impact of EN. Hence for simple one- and two-dimensional systems, we solve Eq. (5) explicitly. Substituting $\tilde{A}$, $\tilde{C}$, $\tilde{D}$ with their expression, we have

$$D = \begin{pmatrix} AC' + C'A^T + \alpha^T C_2^T + C_2\alpha & AC_2 + \alpha C_3 + C_2\beta \\ C_2^T A^T + C_3\alpha^T + \beta C_2^T & \beta C_3 + C_3\beta \end{pmatrix}. \tag{A6}$$

Hence

$$C_3 = -\tfrac{1}{2}D_E\beta^{-1}, \tag{A7}$$

$$\alpha C_3 + AC_2 + C_2\beta = 0, \tag{A8}$$

$$(AC' + C_2\alpha) + (AC' + C_2\alpha)^{\mathrm{T}} + D = 0. \tag{A9}$$

Comparing Eq. (A9) and $AC + CA^{\mathrm{T}} + D = 0$, we have

$$C' = C - A^{-1}\left(\alpha C_2^T + H\right), \tag{A10}$$

where H is an antisymmetric matrix to be determined.

For the insect outbreak model with EN in the main text, we can solve C' directly from the corresponding equations (A8)–(A10),

$$C_3 = \sigma^2, \tag{A11}$$

$$\alpha C_3 + \lambda C_2 + \beta C_2 = 0, \tag{A12}$$

$$2(\lambda C' + \alpha C_2) + D = 0, \tag{A13}$$

which yields

$$C' = \frac{D}{|2\lambda|} + \frac{\sigma_e^2\alpha^2}{|\lambda(\lambda+\beta)|}. \tag{A14}$$

This is Eq. (7) in the main text.

APPENDIX B: FROM CHEMICAL MASTER EQUATIONS TO CHEMICAL LANGEVIN EQUATIONS

In this section, we briefly summarize how chemical master equations can be approximated by chemical Langevin equations (CLEs) for reasonably large systems under a limited span of time [42,70]. Consider a chemical reaction system with N species $S_1,\ldots,S_N$ and M reactions $R_1,\ldots,R_M$. Assume that the system is dilute and well stirred inside a volume Ω. Denote the number of species as X; the evolution of joint probability density of X is described by the following chemical master equation:

$$\frac{\partial P(X,t|x_0,t_0)}{\partial t} = \sum_{m=1}^{M}[a_m(X-\nu_m)P(X-\nu_m,t|X_0,t_0) - a_m(X)P(X,t|X_0,t_0)]. \tag{B1}$$

Here, ν_m is the state change vector of reaction m. The corresponding chemical Langevin equation is

$$X(t+dt)-X(t) = \sum_{m=1}^{M}\nu_m a_m[X(t)]dt + \sum_{m=1}^{M}\sqrt{a_m[X(t)]}\sqrt{dt}N_m(t), \tag{B2}$$

where $N_m(t)$ is the noise with standard Gaussian distribution. Comparing with Eq. (1) in the main text, we have

$$A = \frac{\partial}{\partial X}\left\{\sum_{m=1}^{M}\nu_m a_m[X(t)]\right\}, \tag{B3}$$

$$B = \sum_{m=1}^{M}\nu_m\sqrt{a_m[X(t)]}. \tag{B4}$$

The steady state Jacobean matrix and diffusion matrix can be calculated from the above equations.

The CLE of the insect outbreak model with EN imposed on growth rate is

$$\dot{X} = \eta(t)X - \frac{aX^2}{\Omega} - \frac{\Omega b(X/\Omega)^2}{1+(X/\Omega)^2} + \sqrt{\eta(t)X}\xi_1(t) - \sqrt{\frac{aX^2}{\Omega}}\xi_2(t) - \sqrt{\frac{\Omega b(X/\Omega)^2}{1+(X/\Omega)^2}}\xi_3(t), \tag{B5}$$

where $X(t)\equiv\Omega x(t)$ is the population of the budworm, Ω the system size, $\eta(t)$ the Gaussian extrinsic noise with mean 1 and variance σ_e^2, and $\xi_i(t)$, $i=1,2,3$ is standard Gaussian white noise.

The CLE of the toggle switch model with EN imposed on degradation rates is

$$\frac{dX}{dt} = a_1\Omega\left[a_0+\frac{1-a_0}{1+(Y/\Omega)^{n1}}\right] - \eta(t)X + \sqrt{a_1\Omega\left[a_0+\frac{1-a_0}{1+(Y/\Omega)^{n1}}\right]}\xi_1(t) - \sqrt{\eta(t)X}\xi_2(t), \tag{B6}$$

$$\frac{dY}{dt} = a_2\Omega\left[a_0+\frac{1-a_0}{1+(X/\Omega)^{n2}}\right] - \eta(t)Y + \sqrt{a_1\Omega\left[a_0+\frac{1-a_0}{1+(X/\Omega)^{n1}}\right]}\xi_3(t) - \sqrt{\eta(t)Y}\xi_4(t), \tag{B7}$$

where $X=\Omega x$ and $Y=\Omega y$ are protein numbers, $\eta(t)$ the fluctuating degradation rate of proteins with mean 1 and variances σ_e^2, and $\xi_i(t)$, $i=1,\ldots,4$ is independent standard Gaussian white noise.

APPENDIX C: STOCHASTIC SIMULATION WITH EXTRINSIC NOISE

The stochastic simulations for systems with only IN are performed by the Gillespie algorithm [71,72]. The variant algorithm [32,44] is used to simulate systems with EN. EN is introduced as a fluctuating parameter as described in the main text. The trajectory of EN is simulated according to Eq. (4) with a suitable time step dt using the Euler method [45]. The population number X is updated according to the propensity which depends on the fluctuating parameter until the elapsed time is larger than dt, then the corresponding parameter in the propensity function is updated by the value of EN in time $t+dt$.

The propensity is derived from the deterministic equations by incorporating a system size Ω through the conventional van Kampen expansion [42]. For example, in the simulation of the insect outbreak model, the propensity functions of each reaction at time t are

$$\eta_t X(t),\quad \frac{aX^2(t)}{\Omega},\quad \Omega\frac{b[X(t)/\Omega]^2}{1+[X(t)/\Omega]^2},$$

where η_t is the fluctuating growth rate at time t. The same method is used in simulations of the toggle switch model and the negative feedback model described in the main text.

[1] M. Scheffer, S. Carpenter, J. A. Foley, C. Folke, and B. Walker, Nature **413**, 591 (2001).

[2] M. Scheffer, S. R. Carpenter, V. Dakos, and E. van Nes, Annu. Rev. Ecol. Evol. Syst. **46**, 145 (2015).

[3] A. D. Barnosky, E. A. Hadly, J. Bascompte, E. L. Berlow, J. H. Brown, M. Fortelius, W. M. Getz, J. Harte, A. Hastings, P. A. Marquet *et al.*, Nature **486**, 52 (2012).

[4] T. M. Lenton, H. Held, E. Kriegler, J. W. Hall, W. Lucht, S. Rahmstorf, and H. J. Schellnhuber, Proc. Natl. Acad. Sci. U. S. A. **105**, 1786 (2008).

[5] T. M. Lenton, Nat. Clim. Change **1**, 201 (2011).

[6] C. Wissel, Oecologia **65**, 101 (1984).

[7] A. N. Gorban, E. V. Smirnova, and T. A. Tyukina, Phys. A (Amsterdam, Neth.) **389**, 3193 (2010).

[8] I. A. Van De Leemput, M. Wichers, A. O. J. Cramer, D. Borsboom, and F. Tuerlinckx, Proc. Natl. Acad. Sci. U. S. A. **111**, 87 (2014).

[9] C. Trefois, P. M. A. Antony, J. Goncalves, A. Skupin, and R. Balling, Curr. Opin. Biotechnol. **34**, 48 (2015).

[10] T. Quail, A. Shrier, and L. Glass, Proc. Natl. Acad. Sci. U. S. A. **112**, 9358 (2015).

[11] M. Scheffer, S. R. Carpenter, T. M. Lenton, J. Bascompte, W. Brock, V. Dakos, J. van de Koppel, I. A. van de Leemput, S. A. Levin, E. H. van Nes, M. Pascual, and J. Vandermeer, Science **338**, 344 (2012).

[12] M. Scheffer, J. Bascompte, W. A. Brock, V. Brovkin, S. R. Carpenter, V. Dakos, H. Held, E. H. van Nes, M. Rietkerk, and G. Sugihara, Nature **461**, 53 (2009).

[13] R. Liu, K. Aihara, and L. Chen, Quant. Biol. **1**, 105 (2013).

[14] L. Dai, D. Vorselen, K. S. Korolev, and J. Gore, Science **336**, 1175 (2012).

[15] S. R. Carpenter, J. J. Cole, M. L. Pace, R. Batt, W. A. Brock, T. Cline, J. Coloso, J. R. Hodgson, J. F. Kitchell, D. A. Seekell *et al.*, Science **332**, 1079 (2011).

[16] P. E. McSharry, L. A. Smith, and L. Tarassenko, Nat. Med. **9**, 241 (2003).

[17] V. Dakos, M. Scheffer, E. H. van Nes, V. Brovkin, V. Petoukhov, and H. Held, Proc. Natl. Acad. Sci. U. S. A. **105**, 14308 (2008).

[18] Y. Neuman, O. Nave, and E. Dolev, Complexity **16**, 58 (2011).

[19] V. Guttal and C. Jayaprakash, Ecol. Lett. **11**, 450 (2008).

[20] T. Zeng, S.-y. Sun, Y. Wang, H. Zhu, and L. Chen, The FEBS journal **280**, 5682 (2013).

[21] L. Chen, R. Liu, Z.-P. Liu, M. Li, and K. Aihara, Sci. Rep. **2**, 342 (2012).

[22] S. H. Strogatz, *Nonlinear Dynamics and Chaos: With Applications to Physics, Biology, Chemistry, and Engineering* (Westview Press, Boulder, CO, 1994).

[23] K. Wiesenfeld, J. Stat. Phys. **38**, 1071 (1985).

[24] D. S. Fisher, Phys. Rev. Lett. **56**, 416 (1986).

[25] A. J. Veraart, E. J. Faassen, V. Dakos, E. H. Van Nes, M. Lürling, and M. Scheffer, Nature **481**, 357 (2012).

[26] L. Rindi, M. Dal Bello, L. Dai, J. Gore, and L. Benedetti-Cecchi, Nature Ecology & Evolution **1**, 0153 (2017).

[27] L. Dai, K. S. Korolev, and J. Gore, Nature **496**, 355 (2013).

[28] C. Boettiger and A. Hastings, J. R. Soc., Interface **9**, 2527 (2012).

[29] T. J. W. Wagner and I. Eisenman, Geophys. Res. Lett. **42**, 10333 (2015).

[30] V. Dakos and J. Bascompte, Proc. Natl. Acad. Sci. U. S. A. **111**, 17546 (2014).

[31] C. Boettiger and A. Hastings, Nature **493**, 157 (2013).

[32] M. Assaf, E. Roberts, Z. Luthey-Schulten, and N. Goldenfeld, Phys. Rev. Lett. **111**, 058102 (2013).

[33] A. Kamenev, B. Meerson, and B. Shklovskii, Phys. Rev. Lett. **101**, 268103 (2008).

[34] F. Sagués, J. M. Sancho, and J. García-Ojalvo, Rev. Mod. Phys. **79**, 829 (2007).

[35] W. Horsthemke and R. Lefever, *Noise-Induced Transitions: Theory and Applications in Physics, Chemistry, and Biology* (Springer, Berlin, Heidelberg, 2006).

[36] M. Samoilov, S. Plyasunov, and A. P. Arkin, Proc. Natl. Acad. Sci. U. S. A. **102**, 2310 (2005).

[37] T.-L. To and N. Maheshri, Science **327**, 1142 (2010).

[38] L. Gammaitoni, I. Nazionale, D. Fisica, and S. Perugia, Rev. Mod. Phys. **70**, 223 (1998).

[39] J. Elf and M. Ehrenberg, Genome Res. **13**, 2475 (2003).

[40] J. Paulsson, Phys. Life Rev. **2**, 157 (2005).

[41] J. Keizer, *Statistical Thermodynamics of Nonequilibrium Processes* (Springer Science & Business Media, Berlin, 2012).

[42] N. G. Van Kampen, *Stochastic Processes in Physics and Chemistry* (Elsevier Science, Amsterdam, 2011).

[43] A. Hilfinger and J. Paulsson, Proc. Natl. Acad. Sci. U. S. A. **108**, 12167 (2011).

[44] V. Shahrezaei, J. F. Ollivier, and P. S. Swain, Mol. Syst. Biol. **4**, 196 (2008).

[45] D. T. Gillespie, Phys. Rev. E **54**, 2084 (1996).

[46] V. Shahrezaei and P. S. Swain, Curr. Opin. Biotechnol. **19**, 369 (2008).

[47] M. J. Dunlop, R. S. Cox, J. H. Levine, R. M. Murray, and M. B. Elowitz, Nat. Genet. **40**, 1493 (2008).

[48] R. A. Horn and C. R. Johnson, *Topics in Matrix Analysis* (Cambridge University Press, Cambridge, 1994).

[49] D. Ludwig, D. D. Jones, and C. S. Holling, J. Anim. Ecol. **47**, 315 (1978).

[50] T. S. Gardner, C. R. Cantor, and J. J. Collins, Nature **403**, 339 (2000).

[51] V. Dakos, S. R. Carpenter, E. H. van Nes, and M. Scheffer, Philos. Trans. R. Soc., B **370**, 20130263 (2015).

[52] J. Shi, T. Li, and L. Chen, Phys. Rev. E **93**, 032137 (2016).

[53] F. Vazquez, C. López, J. M. Calabrese, and M. A. Munoz, J. Theor. Biol. **264**, 360 (2010).

[54] M. Pascual and F. Guichard, Trends Ecol. Evol. **20**, 88 (2005).

[55] J. Garcia-Ojalvo and J. Sancho, *Noise in Spatially Extended Systems* (Springer Science & Business Media, Berlin, 2012).

[56] M. C. Cross and P. C. Hohenberg, Rev. Mod. Phys. **65**, 851 (1993).

[57] Y. Imry and S. Ma, Phys. Rev. Lett. **35**, 1399 (1975).

[58] M. Aizenman and J. Wehr, Phys. Rev. Lett. **62**, 2503 (1989).

[59] P. Villa Martín, J. A. Bonachela, and M. A. Muñoz, Phys. Rev. E **89**, 012145 (2014).

[60] R. B. Griffiths, Phys. Rev. Lett. **23**, 17 (1969).

[61] P. V. Martin, J. A. Bonachela, S. A. Levin, and M. A. Muñoz, Proc. Natl. Acad. Sci. U. S. A. **112**, E1828 (2015).

[62] V. Dakos, E. H. van Nes, R. Donangelo, H. Fort, and M. Scheffer, Theor. Ecol. **3**, 163 (2010).

[63] A. Fernández and H. Fort, J. Stat. Mech.: Theory Exp. (2009) P09014.

[64] M. Rietkerk, S. C. Dekker, P. C. De Ruiter, and J. van de Koppel, Science **305**, 1926 (2004).

[65] J. von Hardenberg, E. Meron, M. Shachak, and Y. Zarmi, Phys. Rev. Lett. **87**, 198101 (2001).

[66] S. Kéfi, M. Rietkerk, C. L. Alados, Y. Pueyo, V. P. Papanastasis, A. ElAich, and P. C. De Ruiter, Nature **449**, 213 (2007).
[67] P. S. Swain, M. B. Elowitz, and E. D. Siggia, Proc. Natl. Acad. Sci. U. S. A. **99**, 12795 (2002).
[68] M. B. Elowitz, A. J. Levine, E. D. Siggia, and P. S. Swain, Science **297**, 1183 (2002).
[69] R. J. Prill, R. Vogel, G. A. Cecchi, G. Altan-Bonnet, and G. Stolovitzky, PLoS One **10**, e0125777 (2015).
[70] E. W. J. Wallace, D. T. Gillespie, K. R. Sanft, and L. R. Petzold, IET Syst. Biol. **6**, 102 (2012).
[71] D. T. Gillespie, J. Comput. Phys. **22**, 403 (1976).
[72] D. T. Gillespie, Annu. Rev. Phys. Chem. **58**, 35 (2007).